Energy & Environmental Science

COMMUNICATION

Cite this: *Energy Environ. Sci.*, 2015, **8**, 1998

Received 28th April 2015,
Accepted 27th May 2015

DOI: 10.1039/c5ee01314c

www.rsc.org/ees

A monolithic device for CO_2 photoreduction to generate liquid organic substances in a single-compartment reactor†

Takeo Arai,[ab] Shunsuke Sato[ab] and Takeshi Morikawa[ab]

A solar to chemical energy conversion efficiency of 4.6% was demonstrated for CO_2 photoreduction to formate utilizing water as an electron donor under simulated solar light irradiation to a monolithic tablet-shaped device. The simple CO_2 photoreduction system was realized by exploiting the effect of the carbon substrate on selective CO_2 reduction in the presence of oxygen and selective H_2O oxidation over IrO_x catalysts in the presence of formate.

The development of clean energy sources and CO_2 recycling are crucial approaches to the depletion of fossil resources and climate change induced by an increase in CO_2 emissions; solar energy is an ideal and realistic way to achieve these goals. Direct photoconversion from CO_2 to chemical fuels or organic raw materials for chemical products using water is an ultimate way to realize a sustainable carbon-neutral society. Interest in the direct solar reduction of CO_2 to liquid organic substances has grown due to the higher energy density and accessible storage advantages compared with hydrogen energy. However, direct solar reduction of CO_2 to liquid organics by electrons and protons extracted from water molecules, similar to photosynthesis in plants, has been considered much more difficult than the hydrogen generation reaction. The CO_2 molecule is highly stable, so that challenges to the realization of photoinduced CO_2 recycling using water include the higher potential required for CO_2 reduction than that of hydrogen generation and the low product selectivity in the presence of water. For example, the potentials for CO_2 reduction to CO and formic acid were calculated from the Gibbs free energy change to be −0.10 V (*vs.* SHE) and −0.17 V (*vs.* SHE). There have been several reports on highly efficient catalysts for selective CO_2 photoreduction;[1–4] however, they required a sacrificial reagent as an electron donor to facilitate CO_2 reduction. More importantly, electrical coupling of reactions in a closed system, in which selective water oxidation to extract electrons and selective CO_2 reduction are functionally coupled, is extremely difficult. Few studies on CO_2 photoreduction utilizing water as an electron donor have been reported for semiconductor photocatalysts;[5–8] however, some of them were conducted with an external electrical or chemical bias to assist the reaction, and others were active only under ultraviolet light irradiation. While in the case of complex catalysts, other molecules as sacrificial electron donors are required in place of H_2O to facilitate the reaction. Recently, we reported a solar-to-chemical conversion efficiency of 0.14% for formate generation without an external electrical bias through the combination of a photocathode consisting of a p-type semiconductor, zinc-doped indium phosphide (InP), coated with a $[Ru\{4,4'\text{-di}(1H\text{-pyrrolyl-3-propylcarbonate})2,2'\text{-bipyridine}\}(CO)_2]_n$ polymer (RuCP)[9] catalyst for CO_2 reduction and a $SrTiO_3$ photoanode for water oxidation in a two-compartment reactor separated by a proton exchange membrane, in which water is utilized as both an electron donor and a proton source.[10,11] However, this system should be improved further for practical application. Solar CO_2 recycling requires not only high efficiency and selectivity, but also consideration of the design of simplified low-cost systems. The reduction of CO_2 to formate using a CO_2 electrolyzer equipped with an indium electrode and a Si photovoltaic cell has also been reported.[12] However, an applied voltage of 4–5 V is necessary to operate the CO_2 electrolyzer due to the substantial negative potential for CO_2 reduction over the indium electrode.[12,13] The solar-to-chemical energy conversion efficiency of the system was less than 2%, while the solar power conversion efficiency was 8–9% because the combination of the CO_2 electrolyzer and photovoltaic cells is accompanied by a potential drop due to various resistances (resistances in the solar cell, between the solar cell and the electrode, and permeance at the proton exchange membrane) and also requires a complicated potential transformer for impedance matching. These issues could be overcome using a monolithic tablet-shaped device, which composed of a light absorber, a cathode for CO_2 reduction and an anode

[a] *Toyota Central R&D Labs., Inc., 41-1 Yokomichi, Nagakute, Aichi 480-1192, Japan. E-mail: takeo-arai@mosk.tytlabs.co.jp*
[b] *JST, ACT-C, 4-1-8 Honcho, Kawaguchi, Saitama 332-0012, Japan*

† Electronic supplementary information (ESI) available: Experimental procedure, current–potential characteristics for various measurements, current efficiency for formate production and a simulated solar light spectrum. See DOI: 10.1039/c5ee01314c

for H_2O oxidation. The device is an independent standalone system immersed in a single-compartment reactor filled with water and CO_2. Furthermore, this device is applicable on a large scale by simply setting the devices in an array configuration because the impedance loss caused by scale-up is very small and determined by the direction of tablet thickness. It is also advantageous that replacement of the catalytic components is easier and cheaper.

In the present study, we demonstrate a simple CO_2 photoreduction reaction that utilizes a monolithic tablet-shaped device. The device is composed of a porous ruthenium complex polymer (p-RuCP) as a CO_2 reduction catalyst, iridium oxide (IrO_x) as a water oxidation catalyst, and a triple-junction of amorphous silicon-germanium (SiGe-jn, Fig. S1, ESI†) as a light absorber. p-RuCP was developed by chemical polymerization of RuCP on a porous carbon substrate (see the ESI†) and connected to the stainless steel side (narrower bandgap side of the junction) of the SiGe-jn. An IrO_x nanocolloid containing no organic substances was synthesized according to a previously reported method[14] and coated on the indium tin oxide (ITO) surface of the SiGe-jn (see the ESI†). These components were functionally coupled to realize CO_2 photoreduction with a high solar-to-chemical conversion efficiency in a single-compartment reactor. Two essential technologies were developed to realize the monolithic tablet-shaped device for CO_2 photoreduction; selective CO_2 reduction, even in the presence of H_2O and O_2, and selective H_2O oxidation, even in the presence of organic substances. Without separation functions, such as in the photosynthesis of plants, the organic substances produced from CO_2 in a liquid phase can be re-oxidized and competes with the H_2O oxidation to O_2 reaction. This is also the case for the other side reaction, in which H^+ and O_2 produced from H_2O can be reduced and compete with the CO_2 reduction reaction in a single compartment reactor. Both these reactions cancel the products generated at both sides; therefore, selective CO_2 reduction and H_2O oxidation are necessary for the artificial photosynthesis system to produce liquid chemicals from CO_2 and H_2O in a single-compartment reactor.

The first key technology is the selective CO_2 photoreduction in aqueous media, which was established using the semiconductor–metal-complex hybrid system. We have previously reported the combination of a band-controlled semiconductor for visible-light excitation with a metal-complex to catalyze selective CO_2 reduction, in which photoexcited electrons are transferred from the conduction band of the semiconductor to the lowest unoccupied molecular orbital (LUMO) of the metal-complex catalyst within tens of picoseconds, which resulted in highly selective CO_2 photoreduction.[15,16] Because the concept of the semiconductor–metal-complex hybrid catalyst is highly versatile, we have constructed the InP/RuCP photocathode catalyst for CO_2 reduction.[17]

The CO_2 reduction potential (E_{CR}) of p-RuCP was estimated to be −0.18 V (*vs.* RHE) (Fig. S2 and Table S1, ESI†), which is substantially lower than that of metal electrodes. For example, the CO_2 reduction potential for formate generation over an indium electrode was reported to be −0.90 V (*vs.* RHE).[13] This is the advantage of using a metal-complex catalyst, but there still remain issues such as the competing reduction reaction of O_2 evolved simultaneously over the water-oxidation site with the CO_2 reduction reaction over InP/RuCP. O_2 is more easily reduced than CO_2 and the elimination of O_2 is thus necessary for CO_2 reduction using a metal complex catalyst.

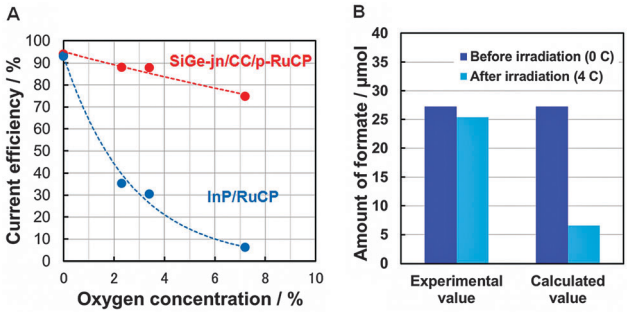

Fig. 1 (A) Current efficiency for formate formation as a function of oxygen concentration in CO_2 flow over SiGe-jn/CC/p-RuCP and InP/RuCP photocathodes under light irradiation for 1 h in 0.1 M phosphate buffer electrolyte. (B) Amount of formate observed before and after photodegradation over the IrO_x/SiGe-jn photoanode.

As evidence, the current efficiency η_C, for formate formation over InP/RuCP in the presence of O_2 is shown in Fig. 1A (see Table S2, ESI,† for details). The InP/RuCP photocathode was used as the working electrode in a three-electrode configuration. The Pt wire and a Hg/Hg_2SO_4 electrode were used as counter and reference electrodes, respectively. 0.1 M phosphate buffer was used as the electrolyte. Gaseous CO_2 containing various concentrations of oxygen was continuously bubbled into the reactor during the reaction, and the CO_2 photoreduction reaction was conducted at +0.21 V (*vs.* RHE) for 1 h. η_C was significantly decreased from 93% (at 0% O_2) to 6% (at 7% O_2) with an increase in the oxygen concentration due to selective O_2 reduction ($O_2 \rightarrow O_2^-$) competing with CO_2 reduction. Therefore, a system was developed to enhance the CO_2 reduction selectivity over RuCP, even in the presence of O_2. A porous carbon cloth (CC) sheet made of carbon fiber was applied, which possesses a low activity for hydrogen generation (Fig. S3, ESI†), and a surface area that is two orders of magnitude larger than that of the flat and smooth surface of a conventional semiconductor film. η_C for formate formation over RuCP coated onto CC (CC/p-RuCP) is also shown in Fig. 1A. CO_2 photoreduction reaction was conducted at +1.41 V (*vs.* RHE). An η_C of 76% was observed, even in the presence of 7% O_2. Comparison of the current–potential characteristics of CC under Ar and CO_2 atmospheres suggested preferential adsorption of CO_2 on the CC (Fig. S4, ESI†). It was thus assumed that gaseous CO_2 in aqueous solution was concentrated adjacent to the CC on which RuCP was polymerized. When the RuCP was applied onto the surface of the stainless-steel side (lower bandgap side) of the SiGe-jn, where H_2 generation is preferential (Fig. S3, ESI†), η_C for formate generation was only 0.3%, while it significantly improved to 94 ± 5% when using CC/p-RuCP (Table S3, ESI†).

The second key technology is highly selective H_2O oxidation, even in the presence of formate. Photoreduction of CO_2 to liquid organic products in a single-compartment cell is difficult because the products accumulated in the liquid phase can be re-oxidized to CO_2 on the surface of water oxidation catalysts

such as TiO_2, as previously reported.[11] Iridium oxide, an excellent catalyst for H_2O oxidation,[18] is reported to oxidize formic acid on Ti/IrO_2 electrodes in perchloric acid.[19] In the present study, formate was not decomposed in the oxidation reaction over the IrO_x catalyst in a phosphate buffer solution. Fig. 1B shows the photodegradation of formate over the IrO_x/SiGe-jn photoanode performed in 0.1 M phosphate buffer electrolyte containing *ca.* 27 μmol (*ca.* 1.4 mM) of formate with a three-electrode configuration at −0.25 V (*vs.* RHE). The bias voltage was set at the operation point of the present device estimated with a two-electrode configuration (details are provided later). Even though the total charge of 4 C observed during the photoanodic reaction over the IrO_x/SiGe-jn photoanode was sufficient to decompose *ca.* 21 μmol formate (calculated value in Fig. 1B), the amount of formate decreased was negligible, which indicates that the IrO_x catalyst has very low activity for the photodegradation of formate. It was also reported that the current efficiency for formate degradation over Ti/IrO_2 in a perchloric acid electrolyte decreased from over 90% to less than 10%, according to the decrease in the concentration of formate from *ca.* 550 mM to *ca.* 30 mM, which indicates that the applied current exceeds the mass transport limit of formate.[17] Therefore, it is supposed that the anodic photocurrent over the IrO_x/SiGe-jn photoanode also exceeded the mass transport of formate on the surface of the IrO_x catalyst and generated oxygen from water. The negligible photodegradation of formate over the IrO_x/SiGe-jn photoanode was also observed in sulfate, borate and carbonate solutions (Fig. S5, ESI†).

SiGe-jn was selected as the semiconductor for photoexcitation, as employed in the previous report.[20] SiGe-jn has an open circuit voltage (V_{OC}) of 2.1 V, which is thermodynamically adequate to oxidize water and extract electrons (approximately 1.4 V), and the p–i–n and tunnel junctions in SiGe-jn facilitate the charge separation and transfer of photoexcited electrons and holes.[21] The conduction band minimum (E_{CBM}) of SiGe-jn was estimated to be −0.52 V (*vs.* RHE) from the current–potential characteristics (Fig. S6, ESI†). The E_{CBM} of SiGe-jn is more negative than the E_{CR} of −0.18 V (*vs.* RHE, see Fig. S2, ESI†) over p-RuCP; therefore, electron transfer from SiGe-jn in a photoexcited state to p-RuCP is thermodynamically possible. Furthermore, the valence band maximum (E_{VBM}) of SiGe-jn was estimated to be 1.58 V (*vs.* RHE) by subtracting V_{OC} from E_{CBM}. The onset potential estimated from the current–potential curve for water oxidation (E_{WO}) over IrO_x was also estimated to be 1.5 V (*vs.* RHE) (Fig. S7, ESI†). Thus, the E_{VBM} of SiGe-jn is also more positive than the E_{WO} over IrO_x, so that IrO_x/SiGe-jn can facilitate H_2O oxidation. The semiconductor–metal-complex hybrid system employs a technical advantage of the Ru-complex catalyst, *i.e.*, a low potential required for CO_2 reduction; therefore, the system using the SiGe-jn can demonstrate CO_2 reduction to formate coupled with water oxidation reaction with a very low voltage of less than 2.1 V.

Based on these two key technologies, the IrO_x/SiGe-jn/CC/p-RuCP monolithic tablet-shaped device was constructed. A schematic illustration of the device is shown in Fig. 2A. The CO_2 photoreduction reaction was conducted by immersing the device in an aqueous phosphate buffer solution saturated with

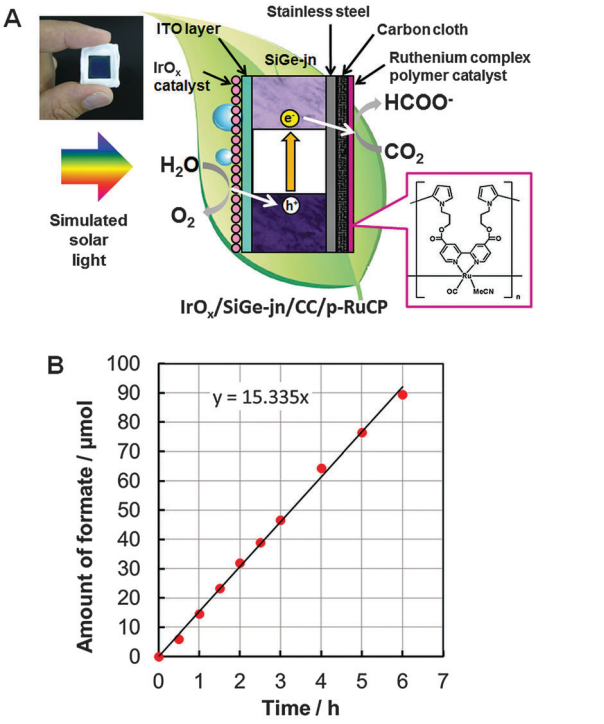

Fig. 2 (A) Schematic illustration of the IrO_x/SiGe-jn/CC/p-RuCP monolithic tablet-shaped device for CO_2 photoreduction. (B) Time course for the generation of formate during the CO_2 photoreduction reaction using IrO_x/SiGe-jn/CC/p-RuCP under simulated solar light irradiation (1 sun, AM1.5, 0.25 cm^2). The IrO_x/SiGe-jn/CC/p-RuCP monolith was immersed in a single-compartment quartz reactor filled with CO_2-saturated phosphate buffer solution (pH 6.4).

gaseous CO_2 (pH 6.4) in a single-compartment reactor under irradiation with solar simulated light (1 sun, AM1.5, Fig. S8, ESI†). Formate as a liquid organic substance was generated from only CO_2 and H_2O raw materials using sunlight as an energy source. The time course for the generation of formate during the CO_2 photoreduction reaction using the monolithic device with the best performance under simulated solar light irradiation (through a square-shaped slit of 0.25 cm^2) is shown in Fig. 2B. Formate was generated continuously during irradiation for 6 h and the solar-to-chemical conversion efficiency was calculated to be 4.6% from the rate of formic acid generation (μmol HCOOH s^{-1}) multiplied by the change in Gibbs free energy per mole of formic acid formation from CO_2 and water (at 298 K, ΔG = 270 kJ mol^{-1}) according to a previous report.[22] This result is supported by the photocurrent observed at the operation point shown in the current–potential characteristics of the IrO_x/SiGe-jn photoanode and the CC/p-RuCP cathode in the three-electrode configuration (Fig. S9, ESI†). A similar photocurrent was also observed at zero bias (*vs.* counter electrode) with the two-electrode configuration using the IrO_x/SiGe-jn and CC/p-RuCP electrodes (Fig. S10, ESI†). The solar-to-chemical conversion efficiency for the present CO_2 reduction is comparable to that observed for solar hydrogen production utilizing a similar light absorber[20] and also reached a level comparable to the theoretical maximal photosynthetic energy conversion

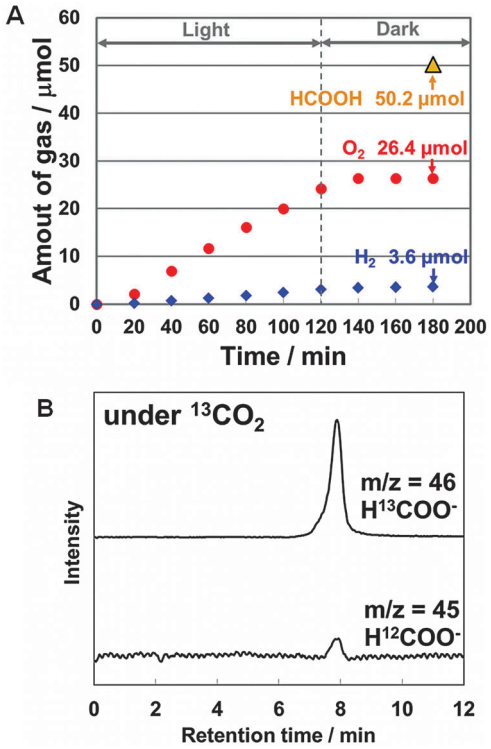

Fig. 3 (A) Experimental verification for formate production from CO_2 and water molecules; time course for oxygen and hydrogen generation during CO_2 photoreduction using a tablet-shaped wireless configuration. The amount of formate was determined at the end of the photoreaction. (B) IC-TOFMS spectra from a tracer experiment utilizing $^{13}CO_2$.

efficiency for C3 crops (*e.g.*, rice and wheat), estimated to be 4.6%.[23] This reaction was also confirmed to be reproducible. The mean value of the solar-to-chemical conversion efficiency utilizing three monolithic devices was 4.3%.

To verify a stoichiometric reaction, the quantity of oxygen molecules generated over IrO_x/SiGe-jn/CC/p-RuCP during CO_2 photoreduction was determined from *in situ* measurements. The experiment was conducted in a flow reactor equipped with a single-compartment Pyrex glass cell and a gas chromatograph. The IrO_x/SiGe-jn/CC/p-RuCP monolithic device was immersed in 0.1 M phosphate buffer saturated with gaseous CO_2 (flow rate 20 mL min^{-1}). A solar simulator equipped with an AM1.5 filter was also used as the light source. The irradiation conditions were different from that used in Fig. 2B due to the experimental setup (see the ESI† for details). During light irradiation, oxygen bubbles were clearly observed at the IrO_x surface. The total amount of oxygen generated after 2 h irradiation was 26.4 μmol (Fig. 3A), which corresponds to 105.6 μmol of photoexcited holes, while 50.2 μmol of formate in the liquid phase and 3.6 μmol of hydrogen in the gas phase were generated simultaneously after 2 h irradiation, which accounts for 107.6 μmol of photoexcited electrons. The amount of electrons was approximately equal to that of photoexcited holes, which strongly suggest that stoichiometric CO_2 reduction is achieved using electrons extracted from water molecules. Furthermore, the ratio of the number of electrons consumed to generate formate to that for the total reduction products was 93%, which is in good agreement with the current efficiency for formate production observed in a half reaction over the SiGe-jn/CC/p-RuCP photocathode (Table S3, ESI†).

In addition, isotope tracer analysis was conducted using the IrO_x/SiGe-jn/CC/p-RuCP device in 0.1 M phosphate buffer saturated with gaseous $^{13}CO_2$ (flow rate 20 mL min^{-1}) to avoid the possibility of experimental error warned by Mul and colleagues.[22] Ion chromatography interfaced with time-of-flight mass spectrometry (IC-TOFMS) was used to clarify the formation of $H^{13}COO^-$ (m/z = 46) (Fig. 3B, mass spectra are shown in Fig. S11, ESI†), which confirmed that the carbon source for formate was the CO_2 molecules. Thus, formate was generated from only CO_2, H_2O and solar energy over the monolithic device.

Conclusions

A monolithic tablet-shaped device was developed for CO_2 photoreduction to liquid organics in a single-compartment cell. CO_2 photoreduction reaction in almost neutral pH aqueous media containing gaseous CO_2 under irradiation of simulated solar light (1 sun, AM1.5) was successfully demonstrated by immersing the monolithic tablet-shaped device composed of a semiconductor–metal-complex hybrid system in a single-compartment reactor. The solar-to-chemical energy conversion efficiency for formate generation reached 4.6% without external electrical and chemical bias voltages, or a membrane for the separation of products. CO_2 photoreduction to formate utilizing H_2O as an electron donor and a proton source was confirmed by the stoichiometry of reduction/oxidation products and isotope tracer analysis. Highly selective CO_2 reduction and water oxidation in the presence of competitive substrates were identified as the primary technological keys that enable the total reaction to occur in a single-compartment reactor. The secondary key is to facilitate electron transfer from the H_2O oxidation catalyst to the CO_2 reduction catalyst by overcoming the slow CO_2 reduction rate over the metal-complex catalyst. These technologies provide a general and paradigm-changing concept for standalone artificial photosynthesis. The efficiency of the present system can be improved by further optimizing the composition of materials and band engineering of semiconductors and metal complexes because the concept of the semiconductor–metal-complex hybrid system is highly versatile.[24–28] Therefore, the development of new semiconductor materials and metal-complex catalysts is crucial for further improvement. Furthermore, since a costly iridium oxide catalyst is impractical, development of a water oxidation catalyst is still important. Formic acid, which was generated in the present system, is an industrially useful organic substance[29] that has the potential to function as a liquid energy carrier with a high density for CO or H_2, and as a chemical form for CO_2 fixation with high density. Direct formic acid fuel cells[30] and the utilization of formic acid as a hydrogen carrier for fuel cells[31] have been investigated. A recent report indicated that methanol can be synthesized *via* disproportionation of formic acid catalyzed by a molecular iridium species.[32] As an extension,

appropriate replacement of the catalysts in the present system could lead to the direct generation of alcohol.[33]

Acknowledgements

The authors thank Dr R. Asahi for useful discussion. The authors also thank M. Yamamoto, M. Asaoka, H. Uchiyama, N. Kawahara, and M. Kondo for technical assistance.

Notes and references

1 J. Hawecker, J.-M. Lehn and R. Ziessel, *J. Chem. Soc., Chem. Commun.*, 1983, 536–538.
2 Y. Tamaki, K. Koike, T. Morimoto and O. Ishitani, *J. Catal.*, 2013, **304**, 22–28.
3 T. Morimoto, C. Nishiura, M. Tanaka, J. Rohacova, Y. Nakagawa, Y. Funada, K. Koike, Y. Yamamoto, S. Shishido, T. Kojima, T. Saeki, T. Ozeki and O. Ishitani, *J. Am. Chem. Soc.*, 2013, **135**, 13266–13269.
4 S. Sato, T. Morikawa, T. Kajino and O. Ishitani, *Angew. Chem., Int. Ed.*, 2013, **52**, 988–992.
5 M. Halmann, *Nature*, 1978, **275**, 115–116.
6 T. Inoue, A. Fujishima, S. Konishi and K. Honda, *Nature*, 1979, **277**, 637–638.
7 K. Iizuka, T. Wato, Y. Miseki, K. Saito and A. Kudo, *J. Am. Chem. Soc.*, 2011, **133**, 20863–20868.
8 S. Yotsuhashi, H. Hashiba, M. Deguchi, Y. Zenitani, R. Hinogami, Y. Yamada, M. Deura and K. Ohkawa, *AIP Adv.*, 2012, **2**, 042160.
9 S. Chardon-Noblat, A. Deronzier, R. Ziessel and D. Zsoldos, *J. Electroanal. Chem.*, 1998, **444**, 253–260.
10 S. Sato, T. Arai, T. Morikawa, K. Uemura, T. M. Suzuki, H. Tanaka and T. Kajino, *J. Am. Chem. Soc.*, 2011, **133**, 15240–15243.
11 T. Arai, S. Sato, T. Kajino and T. Morikawa, *Energy Environ. Sci.*, 2013, **6**, 1274–1282.
12 J. L. White, J. T. Herb, J. J. Kaczur, P. W. Majsztrik and A. B. Bocarsly, *J. CO_2 Util., 2014,* 7, *1–5.*
13 Z. M. Detweiler, J. L. White, S. L. Bernasek and A. B. Bocarsly, *Langmuir*, 2014, **30**, 7593–7600.
14 Y. Zhao, E. A. Hernandez-Pagan, N. M. Vargas-Barbosa, J. L. Dysart and T. E. Mallouk, *J. Phys. Chem. Lett.*, 2011, **2**, 402–406.
15 S. Sato, T. Morikawa, S. Saeki, T. Kajino and T. Motohiro, *Angew. Chem., Int. Ed.*, 2010, **49**, 5101–5105.
16 K. Yamanaka, S. Sato, M. Iwaki, T. Kajino and T. Morikawa, *J. Phys. Chem. C*, 2011, **115**, 18348–18353.
17 T. Arai, S. Sato, K. Uemura, T. Morikawa, T. Kajino and T. Motohiro, *Chem. Commun.*, 2010, **46**, 6944–6946.
18 S. Trasatti, *Electrochim. Acta*, 1984, **29**, 1503–1512.
19 S. Fierro, L. Ouattara, E. H. Calderon, E. Passas-Lagos, H. Baltruschat and C. Comninelis, *Electrochim. Acta*, 2009, **54**, 2053–2061.
20 S. Y. Reece, J. A. Hamel, K. Sung, T. D. Jarvi, A. J. Esswein, J. J. H. Pijpers and D. G. Nocera, *Science*, 2011, **334**, 645–648.
21 X. Deng and E. A. Schiff, in *Handbook of Photovoltaic Science and Engineering*, ed. A. Luque and S. Hegedus, Wiley, Chichester, England, 2003, pp. 505–565.
22 Z. Chen, T. F. Jaramillo, T. G. Deutsch, A. Kleiman-Shwarsctein, A. J. Forman, N. Gaillard, R. Garland, K. Takanabe, C. Heske, M. Sunkara, E. W. McFarland, K. Domen, E. L. Miller, J. A. Turner and H. N. Dinh, *J. Mater. Res.*, 2010, **25**, 3–16.
23 X.-G. Zhu, S. P. Long and D. R. Ort, *Curr. Opin. Biotechnol.*, 2008, **19**, 153–159.
24 C.-C. Yang, Y.-H. Yu, B. van der Linden, J. C. S. Wu and G. Mul, *J. Am. Chem. Soc.*, 2010, **132**, 8398–8406.
25 K. Sekizawa, K. Maeda, K. Koike, K. Domen and O. Ishitani, *J. Am. Chem. Soc.*, 2013, **135**, 4596–4599.
26 K. Maeda, K. Sekizawa and O. Ishitani, *Chem. Commun.*, 2013, **49**, 10127–10129.
27 M. Schreier, P. Gao, M. T. Mayer, J. Luo, T. Moehl, M. K. Nazeeruddin, S. D. Tilley and M. Grätzel, *Energy Environ. Sci.*, 2015, **8**, 855–861.
28 B. Kumar, J. M. Smieja, A. F. Sasayama and C. P. Kubiak, *Chem. Commun.*, 2012, **48**, 272–274.
29 W. Leitner, *Angew. Chem., Int. Ed. Engl.*, 1995, **34**, 2207–2221.
30 J. Jiang and A. Wieckowski, *Electrochem. Commun.*, 2012, **18**, 41–43.
31 J. F. Hull, Y. Himeda, W.-H. Wang, B. Hashiguchi, R. Periana, D. J. Szalda, J. T. Muckerman and E. Fujita, *Nat. Chem.*, 2012, **4**, 383–388.
32 A. J. M. Miller, D. M. Heinekey, J. M. Mayer and K. I. Goldberg, *Angew. Chem., Int. Ed.*, 2013, **52**, 3981–3984.
33 D. J. Boston, C. Xu, D. W. Armstrong and F. M. MacDonnell, *J. Am. Chem. Soc.*, 2013, **135**, 16252–16255.

